# Glass Transition and Structural Relaxation in Polystyrene/ Poly(2,6-dimethyl-1,4-phenylene oxide) Miscible Blends

**J. M. G. Cowie and S. Harris**

*Department of Chemistry, Heriot-Watt University, Riccarton, Edinburgh, EH14 4AS U.K.*

**J. L. Gómez Ribelles***

*Depto. de Termodinámica Aplicada, Universidad Politécnica de Valencia, P.O. Box 22012, E-46071 Valencia, Spain*

**J. M. Meseguer, F. Romero, and C. Torregrosa**

*Depto. de Física Aplicada, Universidad Politécnica de Valencia, P.O. Box 22012, E-46071 Valencia, Spain*

*Received October 17, 1997; Revised Manuscript Received January 14, 1999*

ABSTRACT: The glass transition and the structural relaxation processes of blends of polystyrene and poly(2,6-dimethyl-1,4-phenylene oxide) have been studied by differential scanning calorimetry. The experimental results were compared with the prediction of a model based on the calculation of the configurational entropy of the sample during the thermal history. The model is fitted to the experimental results, and material parameters independent of the thermal history are obtained. These parameters are used to estimate the length of the cooperativity unit at the glass-transition temperature for each blend and pure polymer.

## Introduction

The existence of a single glass transition is a widely applied criterion of miscibility in a polymer blend. The cooperative conformational rearrangements in a miscible polymer blend should involve the motion of polymer segments pertaining to both components of the blend. This also produces a single main dielectric or dynamic−mechanical, relaxation process with relaxation times that depend on the composition of the blend, whereas in polymer blends that are immiscible the individual relaxation processes of both phases can be observed experimentally, provided the differences in the relaxation times corresponding to each component are high enough. Nevertheless, different experimental techniques can be sensitive to molecular motions in different characteristic length scales. Thus, a blend showing a single glass transition measured using differential scanning calorimetry, DSC, may show a distribution of viscoelastic or dielectric relaxation times which can be considered as the overlapping of the distributions of the relaxation times of two different mobile species corresponding to the two components of the blend when studied using dynamic−mechanical or dielectric spectroscopy.[1] This means that the dielectric technique is able to detect microheterogeneities of the blend in a smaller length scale than can DSC. NMR studies seem to be even more sensitive, reflecting that the two species in a miscible polymer blend can retain their different motional characteristics although different from those of the pure polymers.[2−4]

Blends of polystyrene (PS) and poly(2,6-dimethyl-1,4-phenylene oxide) (PPO) are generally considered to be miscible. The blends show a single glass transition in DSC and a single dielectric and dynamic−mechanical main relaxation, although the transition covers a broader temperature interval than those in the pure polymers. This has been attributed to the microheterogeneity or localized concentration fluctuations in the blend.[5,6]

In this paper, we characterize the DSC behavior of these blends in detail by means of the study of the kinetics of the structural relaxation process. Structural relaxation is the term that describes the process of the approach to an equilibrium state undergone by a glass, held in constant environmental conditions, after its formation history. This process is reflected in the time evolution of several thermodynamic or physical properties such as specific volume or enthalpy.[7−10] One of the techniques frequently used in the study of the kinetics of the structural relaxation is differential scanning calorimetry because it is able to follow the evolution of the enthalpy during the structural relaxation process, the "enthalpy relaxation", through the measurement of the heat capacity of the sample. In DSC experiments, the results consist of a series of heat capacity $c_p(T)$ curves measured in heating scans from a temperature $T_{lower}$ below the glass-transition temperature $T_g$ to a temperature $T_{upper}$ above $T_g$. Prior to this, the sample has been subjected to a thermal treatment that starts at $T_{upper}$ with the sample in equilibrium, and may include an isothermal stage at an annealing temperature $T_a$ for an annealing time $t_a$. When $T_a$ is not too far from the glass-transition temperature, the $c_p(T)$ curve shows a peak that overlaps the glass transition. Thermal histories that combine high cooling rates and low ageing temperatures may produce peaks in $c_p(T)$ on the low-temperature side of the glass transition, normally called sub-$T_g$ peaks. Both types of behavior have been explained in terms of the evolution of the enthalpy during the heating scan because of the structural relaxation process.

These kinds of experiments have been used to detect immiscibility in the case of polymer blends in which the glass transitions of both components are very close to

10.1021/ma971531j CCC: $18.00 
Published on Web 06/04/1999

each other and a DSC scan measured after a quenching of the sample does not reveal the existence of two transitions in the blend even if phase separation exists. In this case the annealing at a temperature $T_a$ below the $T_g$'s of both components produces a $c_p(T)$ curve showing two peaks corresponding to the two phases present in the blend[11,12] if it is immiscible.

The kinetics of the structural relaxation in miscible polymer blends can show significant differences with respect to that of pure amorphous polymers. Cowie and Ferguson[13] found that in a polystyrene/poly(vinyl methyl ether) (PS/PVME) blend the enthalpy change in the isothermal annealing at $T_a$ is smaller in the blend than in the pure components. The same feature was found by Oudhuis and ten Brinke[14] in the PS/PPO blend that is the subject of this work.

Modeling of the structural relaxation process in the case of miscible blends has been used to study the presence of concentration fluctuations. Oudhuis and ten Brinke[14] used the Narayanaswamy−Moynihan (NM) model[15,16] to describe the structural relaxation of the blends of PS and PPO and pure PS and PPO. The main difficulty was that different sets of parameters were necessary to fit the $c_p(T)$ curve measured after different thermal histories. They concluded that the presence of concentration fluctuations influences the structural relaxation kinetics through a range of $T_g$s in the blend, but it was impossible to compare the values of the model parameters of the blends with those of the pure materials. The NM model was also used by Ho and Mijović to analyze the structural relaxation process of blends of poly(methyl methacrylate) and styrene/acrylonitrile copolymers.[17]

In this paper, the glass transition of the PS/PPO system was studied for pure components and three blends with different compositions. Heat capacities of the blends and pure components were measured over a large range of temperatures and for different thermal histories and compared with a configurational entropy model of structural relaxation.[18−20] This model is a modification of the Scherer−Hodge (SH) model.[21,22] The model equations are presented in such a way that the limiting state of the isothermal structural relaxation at a temperature $T_a$ can be assumed to be different from the equilibrium states obtained by extrapolation from the experimental values measured at temperatures above $T_g$.

For a multistep thermal history, $T(t) = T_0 + \sum_{i=1}^{n}(T_i - T_{i-1})h(t - t_{i-1})$ ($h$ being the Heaviside unit step function), the configurational entropy $S_c(T)$ turns out to be[18]

$$S(t) = S_c^{lim}(T(t)) - \sum_{i=1}^{n}[S_c^{lim}(T_i) - S_c^{lim}(T_{i-1})]\phi[u(t) - u(t_{i-1})] \quad (1)$$

where $u(t)$ is a reduced time

$$u(t) = \int_0^t \frac{d\sigma}{\tau(\sigma)} \quad (2)$$

$\tau$ is a relaxation time that will be defined below. $\phi$ is a relaxation function of the Kohlrausch−Williams−Watts (KWW) type[23]

$$\phi(u) = \exp(-u^{\beta}) \quad (3)$$

and $S_c^{lim} = S_c^{lim}(T)$ is the value of the configurational entropy $S_c$ in the completely relaxed state at $T$, i.e., in the limit state of the structural relaxation process for an annealing temperature $T$.

In eq 2, we assume for $\tau$ a dependence on the instantaneous values of configurational entropy and temperature given by the equation

$$\tau(S_c, T) = A \exp\left(\frac{B}{S_c T}\right) \quad (4)$$

Equation 4 is an extension of the Adam and Gibbs[24] expression for the equilibrium relaxation times for nonequilibrium states.

When the configurational entropy $S_c$ in eq 4 has the equilibrium value $S_c^{eq}(T)$, we have

$$\tau[S_c^{eq}(T), T] = \tau^{eq}(T) = A \exp\left[\frac{B}{S_c^{eq}(T)T}\right] \quad (5)$$

and for the configurational entropy in an equilibrium state, the equation

$$S_c^{eq}(T) = \int_{T_2}^{T} \frac{\Delta c_p(\theta)}{\theta}\, d\theta \quad (6)$$

is valid. In this equation, $T_2$ is the Gibbs−DiMarzio transition temperature,[25] $\Delta c_p(T) = c_{pl}(T) - c_{pg}(T)$ is the configurational heat capacity, and $c_{pl}$ is the heat capacity in the liquid state. $c_{pl}(T)$ is a well-defined and experimentally measurable function for temperatures $T > T_g$.

When $S_c^{lim}(T) = S_c^{eq}(T)$. in eq 1, the model equations essentially reduce to those of the SH model.[18,26] Nevertheless it has been shown that in many polymers the fit to the experimental results is greatly improved[18−20,27] when $S_c^{lim}(T)$ is significantly higher than $S_c^{eq}(T)$. An explanation for this feature is that further configurational rearrangements are impossible when the number of configurations available to the polymer segments attains a certain limit. When the isothermal structural relaxation process at a temperature $T$ below the glass transition starts, after the formation of glass, the free volume and the number of conformations available for the polymer segments is relatively high. On the other hand, in the equilibrium state at the temperature $T$, only a few conformational states are possible. In the theoretical limit, at the temperature $T_2$, only one conformational state is available to the polymer chains. It is reasonable to propose that during ageing from the initial state toward equilibrium, and with the progressive decrease of conformational mobility, a situation is reached in which no further rotations around the main-chain bonds are possible even if the material is still not in one of the conformations corresponding to the equilibrium state. Perfect packing of the chains in an amorphous glass can rarely be achieved, and a physical limit is reached when no further reductions in volume can occur because of the inefficient packing. When this limit is reached, the system is in a metastable state, and no further decrease of the configurational entropy is possible under isothermal conditions. To characterize the shape of the function $S_c^{lim}(T)$, i.e., how far the limiting state is from the equilibrium state, it is necessary to introduce new parameters in the model, which in principle is not desirable. The shape of $S_c^{lim}(T)$ has been selected as shown schematically in Figure 1 to

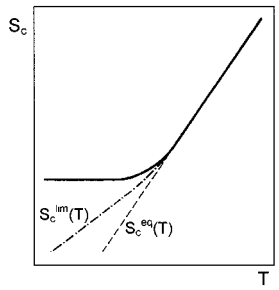


**Figure 1.** Sketch of the configurational entropy corresponding to the liquid state (dashed line), to an experimental cooling scan at a finite cooling rate (solid line), and to the hypothetical line of the limit states of the structural relaxation process (dashed−dotted line).

**Table 1. Glass Transitions Measured as the Intersection Point of the Enthalpy Lines Corresponding to the Liquid and the Glass ($T_{gH}$), Temperature at which the Relaxation Time in Equilibrium is 100 s ($T_g$), and the Density at $T_g$ of the PS/PPO Blends and Pure Polymers**

| PS weight fraction | $T_{gH}$ (K) | $T_g$ (K) | $\rho(T_g)$ (g cm$^{-3}$) |
|---|---|---|---|
| 0 | 487.0 | 488.5 | 1.0249 |
| 16 | 461.0 | 463.0 | 1.0071 |
| 58 | 412.0 | 410.5 | 0.9819 |
| 78 | 394.0 | 393.5 | 0.9741 |
| 100 | 376.5 | 376.5 | 0.9735 |

introduce a single new parameter in the model equations. The slope $dS_c^{lim}(T)/dT$ in the glassy state is $[\Delta c_p(T) - \delta]/T$ [while $dS_c^{eq}(T)/dT = \Delta c_p(T)/T$] where $\delta$ is a fitting parameter. The details of the calculation procedure and the fitting routine have been explained elsewhere.[19,20,27]

## Experimental Section

The PS used was a Polysciences molecular weight standard, with $M_w = 68\,000$ and $M_w/M_n = 1.04$. The sample was dried in a vacuum oven above its $T_g$. No further purification was carried out. Poly(2,6-dimethyl-1,4-phenylene oxide) was obtained from Polysciences. Before use, the polymer was reprecipitated from toluene into methanol. This removed some of the large low-molecular-weight "tail". The molecular weight was then determined from membrane osmometry (in methyl ethyl ketone at 308 K) to be 29 000. The sample was then treated as before.

Blends of PS with PPO containing 16, 58, and 78 wt % of polystyrene were prepared by co-dissolution in toluene followed by precipitation into methanol (see Table 1). The blends were dried in a vacuum oven at 377 K overnight to remove residual solvent before use. Samples were also cycled several times to temperatures several degrees above the $T_g$ of the blends, prior to use. This treatment ensured that there was no residual solvent in the blend, as test samples treated in this way showed only the spectra expected from the blend components when examined using Fourier transform infrared spectroscopy, FTIR.

DSC measurements on samples of the pure polymers and the three blends were performed in a Perkin-Elmer DSC2 calorimeter. Only a single sample for each blend and pure polymer was used in this work. Each sample was subjected to different thermal treatments consisting of the following: an isothermal stage at a temperature $T_{upper}$ above its glass-transition temperature $T_g$, a cooling period at 40 °C/min to the annealing temperature $T_a$, an isothermal stage at this temperature for a time $t_a$, another cooling period at 40 °C/min until the temperature $T_{lower}$ was reached, and finally, a heating scan from $T_{lower}$ to $T_{upper}$ at 20 °C/min. The heat capacity $c_p(T)$ was measured during the heating scan. The scan measured after cooling the sample from $T_{upper}$ to $T_{lower}$ at 40 °C/min, i.e., the one corresponding to the unannealed sample, will be called the reference scan.

## Results and Discussion

The experimental results are expressed as a series of $c_p(T)$ curves determined after thermal histories with different values of $T_a$ and $t_a$. Figures 2−4 show five $c_p(T)$ curves measured after different thermal histories for PS, PPO, and the blend containing 58% PS. The results obtained from the other blends are analogous to those of the 58% blend and are not shown. The annealing temperatures were selected to be around 10 and 15 K below the glass-transition temperature of the sample, determined as the crossing point of the enthalpy lines corresponding to the liquid and glassy states determined from the unannealed scan. Two different annealing times are considered at each annealing temperature. The scan corresponding to the unannealed sample is also shown.

The material parameters of the model were determined for each blend and pure polymer by a simultaneous least-squares fit to the $c_p(T)$ curves shown in Figures 2−4 (the curves selected for the blend containing 16% PS were those measured after thermal treatments with isothermal annealing at 445 K for 120 and 3690 min and at 440 K for 120 and 5520 min and the reference scan; for the blend containing 78% PS, the curves were those corresponding to annealings at 384 K for 120 and 4110 min and at 379 K for 120 and 3970 min and the reference scan).

The correlation existing between parameters $B$, $T_2$, and ln $A$ led us to fix the value of $B$ and determine the rest of the parameters $\delta$, $\beta$, $T_2$, and ln $A$ with the least-squares search routine. The calculation procedure has been explained elsewhere.[20,27] The search routine was conducted for different values of $B$ from the fit with different values of the parameter $B$ for each sample. A linear dependence of the configurational specific heat on temperature was assumed, $\Delta c_p(T) = a_1 + a_2 T$. The results are shown in Tables 2−6. The accuracy of the fit in each sample is nearly the same for the different sets of parameters; i.e., the model-simulated curves for a fixed material calculated with the different sets of parameters are nearly superimposable. Figures 2−4 show the model curve calculated with $B = 500$ J/g as the thick, full line.

The same search routine was conducted using the assumption that $S_c^{lim}(T) = S_c^{eq}(T)$, i.e., keeping $\delta = 0$; now, the least-squares routine allows us to determine the values of the parameters $\beta$, $T_2$, and ln $A$ for each value of $B$. The result with $B = 500$ J/g is shown in Figures 2−4 as the thin, dashed lines. Clearly the results are poorer than in the previous calculations. Thus, it can be said that the model with $S_c^{lim}(T) = S_c^{eq}(T)$ is not able to reproduce the $c_p(T)$ curves measured after different thermal histories with a single set of model parameters, which is a result similar to that reported by Oudhuis and ten Brinke with the NM model.[14]

To return to the model simulation with $S_c^{lim}(T) \neq S_c^{eq}(T)$, the comparison of the model parameters in the

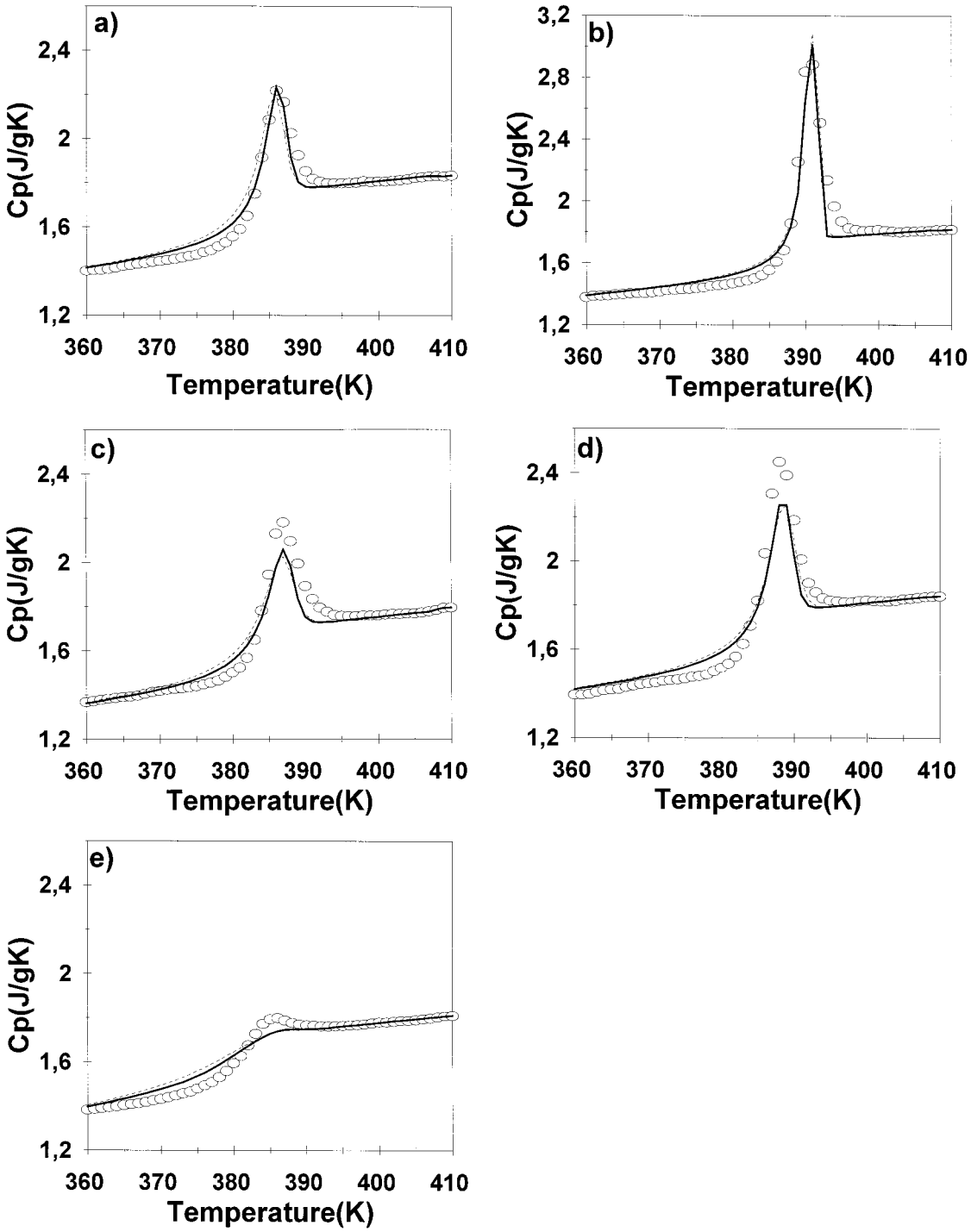


**Figure 2.** Experimental thermograms measured for PS after thermal histories including an isothermal annealing at 367 K for (a) 120 and (b) 3790 min, at 372 K for (c) 120 and (d) 3900 min, and (e) the reference scan. Experimental data are represented as open circles. The solid line represents the prediction of the model with $B = 500$ J/g and the rest of parameters as in Table 2. The dashed line represents the prediction with $\delta = 0$; the model parameters in this case were $B = 500$ J/g, $T_2 = 325.3$, $\ln(A/s) = -39.8$, and $\beta = 0.35$.

different materials again requires the determination of the value of $B$. In PS and PPO, as reported in other polymers, the values of the model parameters are physically reasonable for values of $B$ ranging between 500 and 1000 J/g. Thus, for PPO and $B = 500$ J/g, the preexponential factor $A$ is $0.9\ 10^{-14}$ s, which is the value frequently ascribed to the limit of the relaxation time at high temperature. In PS for the same value of $B$, $A = 2.8\ 10^{-14}$ s. For this value of $B$, the difference $T_g - T_2$ is around 50 K, which is also a very reasonable value when compared to data derived from viscoelastic measurements. When $B$ was increased to 1000 J/g, the value of $A$ decreases to around $10^{-19}$ s and $T_g - T_2$ is around 70 K. These values can be considered as the upper limit of what is physically acceptable, and so, $B = 500$ J/g has been taken as the reference value for comparisons in this work, keeping in mind the great uncertainty in its estimation. As the model with the same value of $B$ reproduces equally well the behavior of PS and PPO, the same value will be assumed for the blends.

Nevertheless, several of the model parameters depend only slightly on the value of $B$ fixed in the search

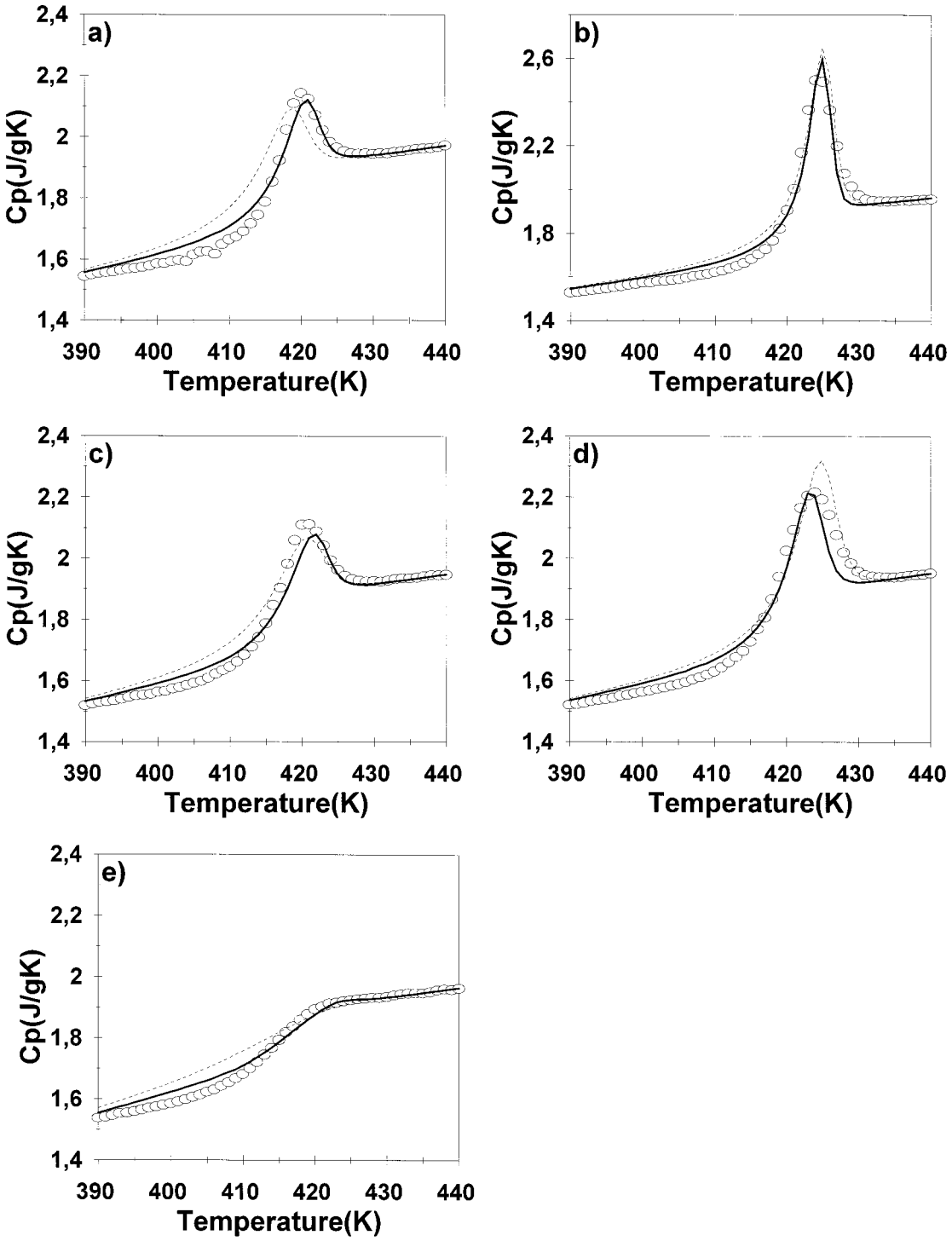


**Figure 3.** Experimental thermograms measured for the blend PS/PPO containing 58% PS after thermal histories including an isothermal annealing at 396 K for (a) 120 and (b) 3900 min, at 401 K for (c) 124 and (d) 3940 min, and (e) the reference scan. Experimental data are represented as open circles. The solid line represents the prediction of the model with $B = 500$ J/g and the rest of parameters as in Table 4. The dashed line represents the prediction with $\delta = 0$; the model parameters in this case were $B = 500$ J/g, $T_2 = 349.3$, $\ln(A/s) = -34.2$, and $\beta = 0.3$.

routine, and the discussion about their values is free of the uncertainty in the estimation of $B$. Thus, the value of $\delta$ is nearly independent of $B$ in any blend or pure polymer, as shown in Tables 2−6. Figure 5 shows that the values of $\delta$ are higher for the blends than would be expected from the values obtained for the pure polymers assuming a simple linear relationship. This feature can be related to the fact that the experimental value of the enthalpy loss, during the isothermal annealing, is smaller in the blends than in the pure components when the difference $T_g - T_a$ is the same.[13,14]

In addition, the value of $\beta$ depends only slightly on the value of $B$ fixed in the least-squares routine. As shown in Figure 6, the value of $\beta$ is lower in the blends than in the pure polymers (in Figure 6, the values of this parameter for $B = 500$ J/g and 1000 J/g show that this conclusion does not depend on the estimate of $B$), which is in line with other results from dynamic−mechanical and dielectric experiments.[28−30] This means that the distribution of relaxation times is broader in

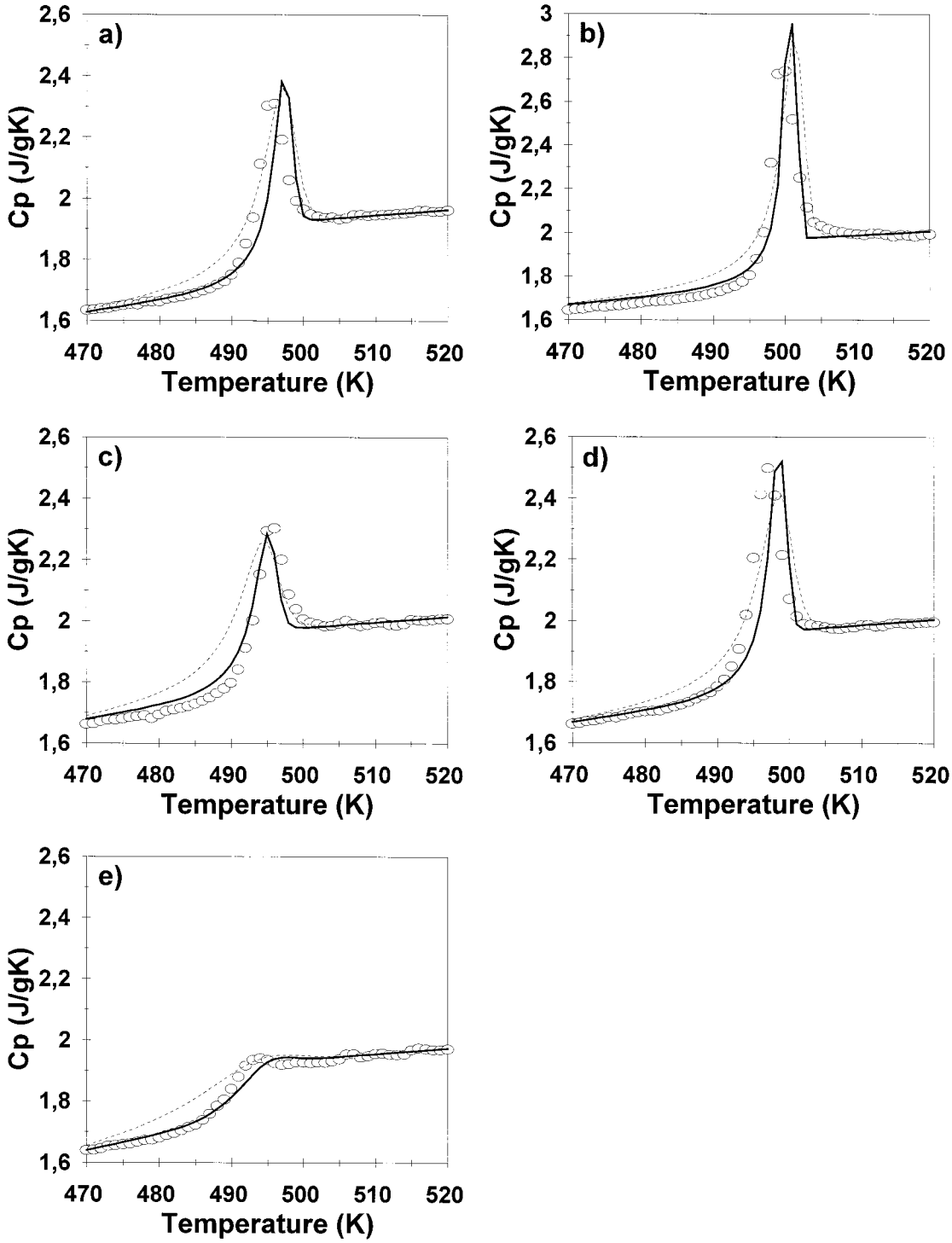


**Figure 4.** Experimental thermograms measured for PPO after thermal histories including an isothermal annealing at 473 K for (a) 90 and (b) 3780 min, at 477 K for (c) 120 and (d) 3840 min, and (e) the reference scan. Experimental data are represented as open circles. The solid line represents the prediction of the model with $B = 500$ J/g and the rest of parameters as in Table 2. The dashed line represents the prediction with $\delta = 0$; the model parameters in this case were $B = 500$ J/g, $T_2 = 420$ K, $\ln(A/s) = -24.0$, and $\beta = 0.41$.

**Table 2. Model Parameters Found for PPO with $S_c^{lim}(T)$ as the Dashed−Dotted Line of Figure 1 for Each Value of $B$**

| $B$ (J/gK) | $\delta$ | $\beta$ | ln $A$ (s) | $T_2$ (K) | $T_g - T_2$ (K) |
|---|---|---|---|---|---|
| 500 | 0.12 | 0.44 | −32.3 | 436 | 53 |
| 1000 | 0.10 | 0.45 | −42.9 | 413 | 76 |
| 1500 | 0.09 | 0.46 | −51.0 | 396 | 93 |
| 2000 | 0.09 | 0.48 | −57.2 | 382 | 107 |

the blends than in the pure polymer components, which can be attributed to both the presence of concentration fluctuations and the different effective $T_g$ for each blend component.[2,3] In a miscible polymer blend, each cooperative rearranging region, CRR, should contain polymer segments pertaining to both components of the blend, so that the relaxation behavior of the blend has the same characteristics as that of a pure polymer, showing a single glass transition and a single main dielectric or dynamic mechanical relaxation process. Nevertheless, the size of the CRR is quite small[31−35] for this blend, as we will show below, and it is reasonable to assume that the proportion of main-chain segments

**Table 3. Model Parameters Found for the PS/PPO Blend Containing 16% PS with $S_c^{lim}(T)$ as the Dashed−Dotted Line of Figure 1 for Each Value of *B***

| *B* (J/gK) | $\delta$ | $\beta$ | ln *A* (s) | $T_2$ (K) | $T_g - T_2$ (K) |
|---|---|---|---|---|---|
| 500 | 0.13 | 0.36 | −28.5 | 406 | 58 |
| 1000 | 0.13 | 0.37 | −39.0 | 384 | 80 |
| 1500 | 0.12 | 0.39 | −46.3 | 369 | 95 |
| 2000 | 0.12 | 0.40 | −52.0 | 356 | 108 |

**Table 4. Model Parameters Found for the PS/PPO Blend Containing 58% PS with $S_c^{lim}(T)$ as the Dashed−Dotted Line of Figure 1 for Each Value of *B***

| *B* (J/gK) | $\delta$ | $\beta$ | ln *A* (s) | $T_2$ (K) | $T_g - T_2$ (K) |
|---|---|---|---|---|---|
| 500 | 0.10 | 0.36 | −27.2 | 355 | 55 |
| 1000 | 0.09 | 0.37 | −37.2 | 331 | 79 |
| 1500 | 0.09 | 0.39 | −41.2 | 313 | 97 |
| 2000 | 0.08 | 0.40 | −49.5 | 299 | 111 |

**Table 5. Model Parameters Found for the PS/PPO Blend Containing 78% PS with $S_c^{lim}(T)$ as the Dashed−Dotted Line of Figure 1 for Each Value of *B***

| *B* (J/gK) | $\delta$ | $\beta$ | ln *A* (s) | $T_2$ (K) | $T_g - T_2$ (K) |
|---|---|---|---|---|---|
| 500 | 0.12 | 0.39 | −27.2 | 343 | 51 |
| 1000 | 0.11 | 0.41 | −37.3 | 322 | 72 |
| 1500 | 0.10 | 0.42 | −44.3 | 307 | 87 |
| 2000 | 0.11 | 0.44 | −50.8 | 296 | 98 |

**Table 6. Model Parameters Found for PS with $S_c^{lim}(T)$ as the Dashed−Dotted Line of Figure 1 for Each Value of *B***

| *B* (J/gK) | $\delta$ | $\beta$ | ln *A* (s) | $T_2$ (K) | $T_g - T_2$ (K) |
|---|---|---|---|---|---|
| 500 | 0.07 | 0.39 | −31.2 | 329 | 47 |
| 1000 | 0.05 | 0.41 | −42.3 | 309 | 72 |
| 1500 | 0.05 | 0.44 | −50.5 | 294 | 84 |
| 2000 | 0.05 | 0.45 | −55.1 | 279 | 97 |

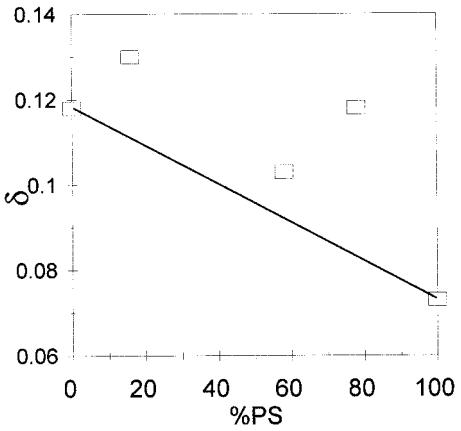


**Figure 5.** Composition dependence of the $\delta$ parameter in the blend. Values obtained with the least-squares routine conducted with $B = 500$ J/g.

of each component inside a CRR may be different from the average composition of the blend, leading to different values of the relaxation time due to the different mobilities of both species. Thus, the distribution of relaxation times in the blend is broader than in the pure components. It is important to note that the model reproduces, more or less with the same accuracy, the DSC results obtained in the case of the blend as in the pure polymers. This means that the concentration fluctuations in the blend are not important enough to make the main assumptions of the model invalid, in particular the use of a single KWW equation characterizing the distribution of relaxation times of the blend. It makes no sense to introduce in the model equations a more complicated shape for the distribution of relaxation times for the blend, such as the superposition of two KWW distributions that would be characteristic of the different mobilities of the two components. From the point of view of the DSC technique or in terms of the length scales being probed by DSC, the blend behaves as if it is homogeneous but more distributed than the pure components.

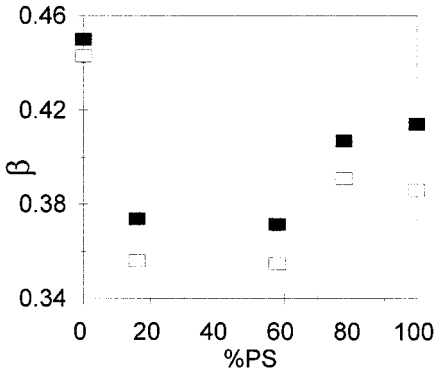


**Figure 6.** Composition dependence of the $\beta$ parameter in the blend. Values obtained with the least-squares routine conducted with $B = 500$ (□) and 1000 J/g (■).

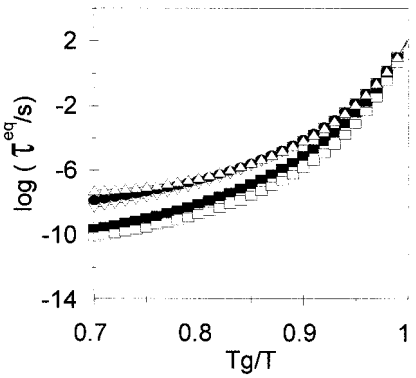


**Figure 7.** Temperature dependence of the relaxation times in equilibrium determined with the model parameters found by the search routine with $B = 500$ J/g in PPO (□) and PS (■) and the blends containing 16% (△), 58% (▽), and 78% (●) PS.

Figure 6 shows that the addition of a small amount of PS to PPO produces a larger decrease in the value of $\beta$ than the addition of a small amount of PPO to PS. The reason for this can be related to the dependence of the glass-transition temperature of the blend on its composition. The curvature of the $T_g$ versus $w_{PS}$ curve (where $w_{PS}$ is the weight fraction of PS), see Figure 9 below, yields higher values of $\partial T_g/\partial w_{PS}$ for low PS contents. Thus, the concentration fluctuations produce larger fluctuations in the glass-transition temperatures in this zone of the blend composition and yield a broader relaxation-time distribution. Our result is in good agreement with NMR studies of polyisoprene/poly(vinylethylene) (PI/PVE) miscible blends,[3] which found that when the higher $T_g$ component content in the blend increases, the distribution of relaxation times is broader because of the greater difference between each effective $T_g$ of the blend components.

The temperature dependence of the relaxation times in equilibrium is another parameter that depends only slightly on the value of *B*, as has been shown in many polymers.[18−20,26,27] The logarithm of the relaxation times in equilibrium conditions log $\tau^{eq}$ is plotted as a function of $T_g/T$ in Figure 7 and shows that the slope is smaller in the blends than in the pure polymers, as a conse-

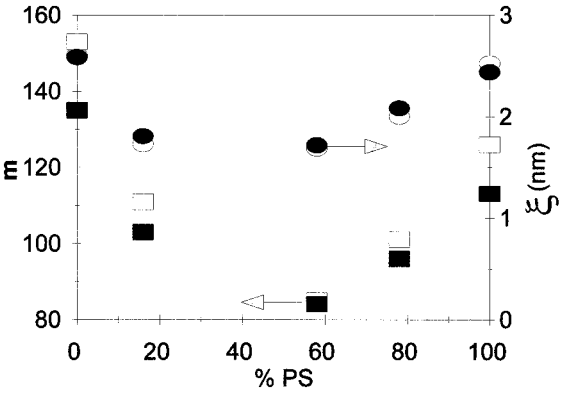


**Figure 8.** Composition dependence of the fragility parameter $m$ in the blend [values obtained with the least-squares routine conducted with $B = 500$ (□) and 1000 J/g (■)] and the correlation length for $B = 500$ (○) and 1000 J/g (●).

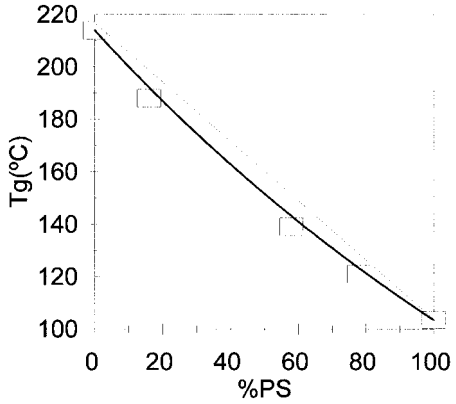


**Figure 9.** Glass-transition temperature of the blends and pure components calculated as the temperature at which the relaxation time in equilibrium is 100 s. The solid line represents the prediction of the Fox equation. See text.

quence of the composition dependence of $T_g - T_2$ and ln $A$. This feature can be discussed in terms of the "fragile−strong" classification proposed by Angell.[34] The fragility parameter "$m$" can be defined through

$$m = \frac{\mathrm{d}\log \tau^{eq}}{\mathrm{d}T_g/T}\Big|_{T_g} \tag{7}$$

The values, calculated for the pure polymers and the blends are shown in Figure 8. It can be said that the blends behave as though they are "stronger" than the pure polymers. In this calculation, the glass-transition temperature of each material has been defined as the temperature for which the equilibrium relaxation time is 100 s. As shown in Table 1, this temperature is very close to the temperature of the intersection of the enthalpy lines corresponding to the liquid and the glassy states. The dependence of this glass-transition temperature on composition (Figure 9) follows the Fox equation

$$\frac{1}{T_g} = \frac{\omega_1}{T_{g1}} + \frac{\omega_2}{T_{g2}} \tag{8}$$

where $\omega_i$ is the weight fraction of component $i$.

The data available from the model fit of the DSC results are enough to get an estimate of the size of the CRR. Donth[33,36] proposed a formula for the volume $V_a$ of the CRR on the basis of his temperature fluctuation theory, which is

$$V_a = \frac{kT_g^2}{\rho\delta T^2}\left(\frac{1}{c_{pg}} - \frac{1}{c_{pl}}\right) \tag{9}$$

where $\rho$ is the density and $\delta T$ is the mean temperature fluctuation in the CRR.

The temperature fluctuation was calculated from the mean fluctuation of ln $\tau$ given by

$$\frac{\delta(\ln \tau)}{\delta T} = \frac{1}{T_g^2}\left[\frac{\mathrm{d}\ln \tau^{eq}}{\mathrm{d}(1/T)}(T_g)\right] \tag{10}$$

and the fluctuation of ln $\tau$ is related to the parameter $\beta$ by the equation

$$\delta(\ln \tau) = \frac{C}{\beta} \tag{11}$$

with $C = 1.04 \pm 0.05$.

The densities at $T_g$ of each blend and pure polymers were obtained from the data reported at 24 °C by Yee,[28] and the expansion coefficients in the glassy state were calculated using the thermal expansion coefficients in the liquid state from the data published by Maconnachie et al.[37] and the Simha−Boyer relationship[38]

$$(\alpha_l - \alpha_g)T_g = 0.113 \tag{12}$$

The correlation length $\xi$ is defined by[36,39]

$$\xi \approx V_a^{1/3}$$

The values of the correlation length for the blends and pure polymers are shown in Figure 8. The correlation lengths found are lower for the blends than for the pure polymers, and all of them are in the range of 1.5−3 nm reported for other polymers.[33,39] However, a correlation length as low as 0.4 nm has been estimated for PS/PPO (50%) from NMR data.[40] The composition dependence of the correlation length is closely related to that of $\beta$ and the fragility parameter $m$. Equations 7 and 9−11 lead to

$$V_a = \frac{2.303^2 m^2 \beta^2}{\rho C^2}\left(\frac{1}{c_{pg}} - \frac{1}{c_{pl}}\right) \tag{13}$$

As the density and the increment of $1/c_p$ in the transition depend monotonically on the composition of the blend, the minimum shown by both $\beta$ and $m$ makes the correlation length pass through a minimum.

## Concluding Remarks

The model used in this work is able to reproduce the DSC structural relaxation behavior of PS-PPO blends and pure PS and PPO with similar accuracy. It has been shown that the model with a single set of parameters is able to reproduce the $c_p(T)$ curves measured after different thermal histories. The values of the parameters of the model determined with $B = 500$ J/g are very reasonable according its physical meaning. Thus, the limit of the relaxation times at high temperatures is around $10^{-14}$ s, and the difference $T_g - T_2$ is approximately 50 K. As the modeling of the experimental results leads to a set of material parameters for each blend, it is possible to examine the dependence of each parameter on the blend composition. All of the parameters show a smooth dependence on the composition of

the blend. It can be concluded that the distribution of relaxation times for the blends is broader than for the pure polymers, and this has been ascribed to the concentration fluctuations in the blend. The blends are shown to be stronger using Angell's definition and to have a smaller correlation length (in the Donth sense) than the pure polymers.

**Acknowledgment.** The work of the group of the Universidad Politécnica de Valencia was partially supported by CICYT through the Project MAT94-0596.

## References and Notes

(1) Alvarez, F.; Alegría, A.; Colemenro, J. *Macromolecules* **1997**, *30*, 597.
(2) Chung, G. C.; Kornfield, J. A.; Smith, S. D. *Macromolecules* **1994**, *27*, 964.
(3) Chung, G. C.; Kornfield, J. A.; Smith, S. D. *Macromolecules* **1994**, *27*, 5729.
(4) Arendt, B. H.; Krishnamoorti, R.; Kornfield, J. A.; Smith, S. D. *Macromolecules* **1997**, *30*, 1127.
(5) MacKnight, W. J.; Karasz, F. E.; Fried, J. R. *Polymer Blends*; Academic Press: New York, 1978.
(6) Fried, J. R. *Developments in Polymer Characterization*; Applied Science: London, 1983.
(7) Scherer, W. *J. Non-Cryst. Solids* **1990**, *123*, 75.
(8) Hodge, I. M. *J. Non-Cryst. Solids* **1994**, *169*, 211.
(9) McKenna, G. B. *J. Res. Natl. Inst. Stand. Technol.* **1994**, *99*, 169.
(10) Hutchinson, J. M. *Prog. Polym. Sci.* **1995**, *20*, 703.
(11) ten Brinke, G.; Grooten, R. *Colloid Polym. Sci.* **1989**, *267*, 992.
(12) Ellis, T. S. *Macromolecules* **1990**, *23*, 1494.
(13) Cowie, J. M. G.; Ferguson, R. *Macromolecules* **1989**, *22*, 2312.
(14) Oudhuis, A. A. C. M.; ten Brinke, G. *Macromolecules* **1992**, *25*, 698.
(15) Narayanaswamy, O. S. *J. Am. Ceram. Soc.* **1971**, *54*, 491.
(16) Moynihan, C. T.; Macedo, P. B.; Montrose, C. J.; Gupta, P. K.; DeBolt, M. A.; Dill, J. F.; Dom, B. E.; Drake, P. W; Easteal, A. J.; Elterman, P. B.; Moeller, R. P; Sasabe, H. *Ann. N. Y. Acad. Sci.* **1976**, *279*, 15.
(17) Ho, T.; Mijović, J. *Macromolecules* **1990**, *23*, 1411.
(18) Gómez Ribelles, J. L.; Monleón Pradas, M. *Macromolecules* **1995**, *28*, 5867.
(19) Gómez Ribelles, J. L.; Monleón Pradas, M.; Más Estellés, J.; Vidaurre Garayo, A.; Romero Colomer, F.; Meseguer Dueñas, J. M. *Polymer* **1997**, *38*, 963.
(20) Brunacci, A.; Cowie, J. M. G.; Ferguson, R.; Gómez Ribelles, J. L.; Vidaurre, A. *Macromolecules* **1996**, *29*, 7976.
(21) Scherer, G. W. *J. Am. Ceram. Soc.* **1984**, *67*, 504.
(22) Hodge, I. M. *Macromolecules* **1987**, *20*, 2897.
(23) Williams, G.; Watts, D. C. *Trans. Faraday Soc.* **1970**, *66*, 80.
(24) Adam, G.; Gibbs, J. H. *J. Chem. Phys.* **1965**, *43*, 139.
(25) Gibbs, J. H.; DiMarzio, E. A. *J. Chem. Phys.* **1958**, *28*, 373.
(26) Gómez Ribelles, J. L.; Monleón Pradas, M.; Más Estellés, J.; Vidaurre Garayo, A.; Romero Colomer, F.; Meseguer Dueñas, J. M. *Miacromolecules* **1995**, *28*, 5878.
(27) Meseguer Dueñas, J. M.; Vidaurre Garayo, A.; Romero Colomer, F.; Más Estellés, J.; Gómez Ribelles, J. L.; Monleón Pradas, M. *J. Polym. Sci., Polym. Phys. Ed.*, in press.
(28) Yee, A. F. *Polym. Eng. Sci.* **1977**, *17*, 213.
(29) Wetton, R. E.; MacKnight, W. J.; Fried, J. R.; Karasz, F. E. *Macromolecules* **1978**, *11*, 158.
(30) Bazuin, C. G.; Rancourt, L.; Villeneuve, S.; Soldera, A. *J. Polym. Sci., Part B: Polym. Phys.* **1993**, *31*, 1431.
(31) Miller, A. A. *J. Chem. Phys.* **1968**, *49*, 1393.
(32) Robertson, R. E. *J. Polym. Sci., Polym. Phys. Ed.* **1979**, *17*, 597.
(33) Donth, E. *J. Non-Cryst. Solids* **1982**, *53*, 325.
(34) Angell, C. A. *J. Non-Cryst. Solids* **1991**, *131*−*133*, 3.
(35) Gómez Ribelles, J. L.; Vidaurre, A.; Cowie, J. M. G.; Ferguson, R.; Harris, S.; McEwen, I. J. *Polymer* **1998**, *40*, 183.
(36) Donth, E. *Relaxation and Thermodynamics in Polymers, Glass Transition*; Akademie Verlag: Berlin, 1992.
(37) Maconnachie, A.; Kambour, R. P.; White, D. M.; Rostami S.; Walsh, D. J. *Macromolecules* **1984**, *17*, 2645.
(38) Boyer, R. F. *J. Macromol. Sci., Phys.* **1973**, *B7*, 487.
(39) Donth, E.; Beiner, M.; Reising, S.; Korus, J.; Garwe, F.; Vieweg, S.; Kahle, S.; Hempel, E.; Schröter, K. *Macromolecules* **1996**, *29*, 6589.
(40) Li, S.; Rice, D. M.; Karasz, F. E. *Macromolecules* **1994**, *27*, 6527.

MA971531J